6-1-1991

Emission from the z = 2 Damped Lyα Absorber Toward Q1215 + 333

Richard Elston
Kitt Peak National Observatory

Jill Bechtold
The University of Arizona

James Lowenthal
The University of Arizona, jlowenth@smith.edu

Marcia Rieke
The University of Arizona

THE ASTROPHYSICAL JOURNAL, 373: L39–L42, 1991 June 1

EMISSION FROM THE $z = 2$ DAMPED Lyα ABSORBER TOWARD Q1215+333[1]

RICHARD ELSTON
Kitt Peak National Observatory, National Optical Astronomy Observatory,[2] Tucson, AZ 85726

AND

JILL BECHTOLD,[3] JAMES LOWENTHAL,[3] AND MARCIA RIEKE
Steward Observatory, The University of Arizona, Tucson, AZ 85721
Received 1991 February 11; accepted 1991 March 14

ABSTRACT

We have detected narrow emission lines at 1.118 μm and 1.456 μm in the spectrum of the $z = 2.606$ quasar Q1215+333, corresponding to [O II] λ3727 and Hβ at $z = 1.9984$, the redshift of a damped Lyα absorber toward this quasar. The intensity of the Hβ line is $7.6 \pm 2 \times 10^{-16}$ ergs cm^{-2} s^{-1}, which corresponds to a line luminosity of 5×10^{42} ergs s^{-1} h_{100}^{-2} ($q_0 = 0.5$). If we assume that the photoionization producing the emission is due purely to massive star formation with a Salpeter initial mass function, we find a total star formation rate of 100 $M_{\odot}$ yr^{-1} h_{100}^{-2}. Given the uncertainty in the initial mass function and cosmological parameters, this star formation rate is very uncertain. However, the star formation rate is well above those inferred from Lyα emission-line searches of similar systems, implying effective destruction of Lyα photons. The intensity of the [O II] λ3727 line is $1.6 \pm 0.3 \times 10^{-15}$ ergs cm^{-2} s^{-1}. The ratio [O II]/H$\beta \approx 2$ and the weakness of the ratio [O III] λ5007/H$\beta < 0.5$ is typical of star formation regions with gas at nearly solar metallicity.

Subject headings: galaxies: individual (1215+333) — quasars

1. INTRODUCTION

While unusual objects such as quasars and radio galaxies are detected to very high redshift, no "normal" isolated galaxies are known at redshifts greater than 1. Absorption lines in the spectra of quasars are the only probes of the distribution, chemical properties, and excitation of diffuse matter in such galaxies in the distant universe. While galaxies producing absorption lines in quasar spectra have been identified at $z < 1$ (Bergeron 1988; Yanny, York, & Williams 1990; Yanny 1990), no certain direct observations have been made of the absorbers at higher redshift. Thus, the nature of high-redshift absorbers is unknown, but for the purposes of this paper we will refer to them as galaxies. The sizes, morphologies, and star formation rates of high-redshift galaxies are important constraints for galaxy formation and evolution.

To determine the nature of high-redshift absorbers several studies have tried to detect the emission from such objects directly. The most popular approach has been to search for Lyα emission from the intervening galaxy (Foltz, Chaffee, & Weymann 1986; Smith et al. 1989; Deharveng, Buat, & Bowyer 1990; Lowenthal et al. 1991). Despite the observation of more than 20 candidates there has been only one weak detection of Lyα emission from the $z = 2.46$ damped Lyα absorber toward Q0836+113 (Hunstead, Pettini, & Fletcher 1990). It is difficult to interpret the weakness of Lyα emission from these systems. Low star formation rates in the intervening galaxies (< 5 $M_{\odot}$ yr^{-1}) are one possibility. On the other hand, since Lyα is multiply scattered, the presence of even a small amount of dust can destroy it. Such amounts of dust are inferred from observations of quasars with and without damped Lyα absorbers (Fall, Pei, & McMahon 1989; Pei, Fall, & Bechtold 1991). Given the problem of Lyα destruction we have decided to search for Hβ, [O II] λ3727 and [O III] λ5007 emission from these systems.

In this paper we present the detection of Hβ and [O II] λ3727 emission from the $z = 2$ damped Lyα absorption-line system in Q1215+333. In the next section we present observations of Hβ and [O II] λ3727 emission with two different instruments. In the final section we use these observations to constrain the source of excitation for the emission-line gas and its metallicity.

2. OBSERVATIONS

Our first observations of Q1215+333 were made with the Cryogenic Spectrometer on the KPNO Mayall 4 m telescope at f/30 on 1990 February 4. The Cryo Spec (Joyce 1991) is a cryogenically cooled long-slit spectrometer using a 58×62 InSb array detector produced by Santa Barbara Research Corporation. The pixel size is $0\farcs9 \times 0.00185$ μm with a spectral coverage from 1.44 to 1.54 μm. We employed the multiple-read noise reduction algorithm of Fowler & Gatley (1990) to reduce the detector noise to about 100 e^- pixel^{-1} rms. With a 300 lines mm^{-1} grating in second order a resolution of about 1000 was achieved. A $2\farcs1$ wide slit was oriented in a north-south direction for these observations with the quasar centered on the slit. Individual background noise–limited observations of 300 s were made on source with sky observations interleaved. The sky spectra were subtracted to achieve dark removal and first-order sky subtraction. The data were then flattened, and residual sky emission was removed by fitting a third-order polynomial in the cross-dispersion direction. The final spectra were then combined by shifting the individual spectra to a common slit position and taking their median. To remove telluric absorption the spectrum was divided by observations of the F9V star 61 Uma.

Figure 1 (Plate 1) shows the two-dimensional spectra of

[1] Observations reported here were obtained with the Multiple Mirror Telescope, a facility operated by the Smithsonian Institution and the University of Arizona.

[2] Operated by the Association of Universities for Research in Astronomy, Inc., under cooperative agreement with the National Science Foundation.

[3] Visiting Astronomers, Kitt Peak National Observatory.

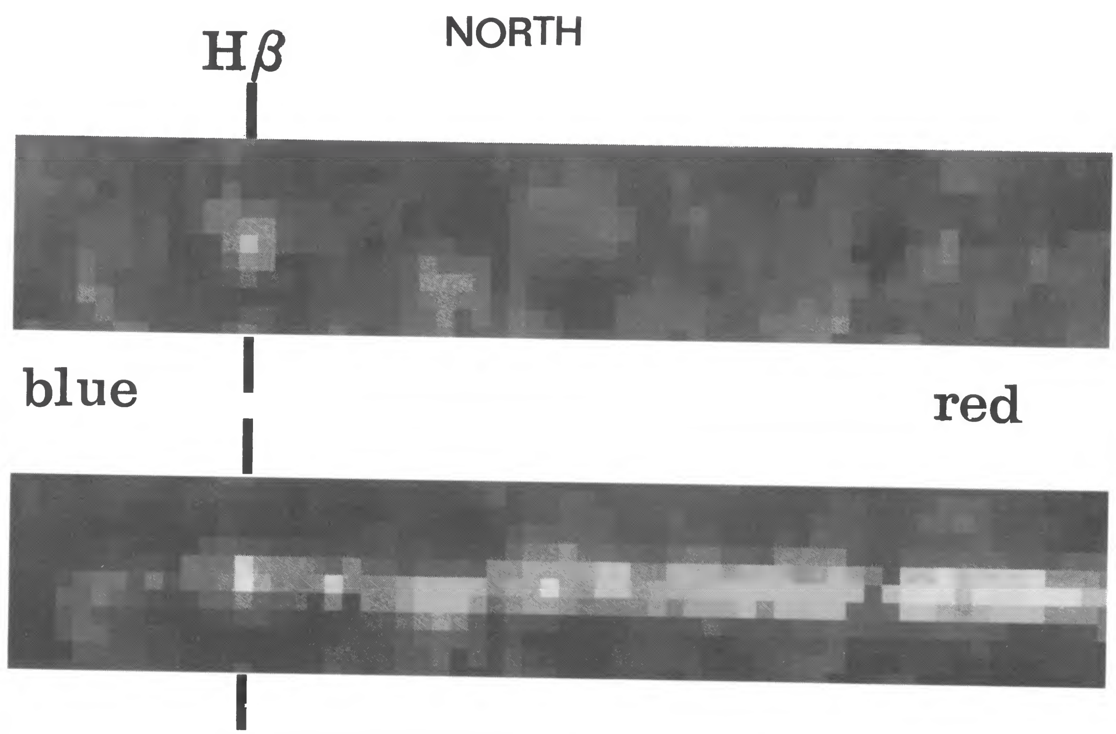

FIG. 1.—Near-IR two-dimensional spectra of Q1215+333. Pixels are 0".9 × 0.0018 μm with north up and red to the right. Lower image shows the full raw spectrum of Q1215+333 obtained with the KPNO 4 m telescope and Cryogenic Spectrometer. Loss of flux toward the left is due to increasing atmospheric absorption toward the blue which has not been corrected for in these two-dimensional spectra so that the noise level appears uniform. Upper image has had a low-order polynomial fitted to the continuum and removed. An emisson line remains at a wavelength which corresponds to Hβ emission from the $z = 2$ damped Lyα absorber toward Q1215+333. Using the statistics of a 3 × 3 pixel box, the emission line is significant at the 4.5 σ level.

ELSTON et al. (see 373, L39)

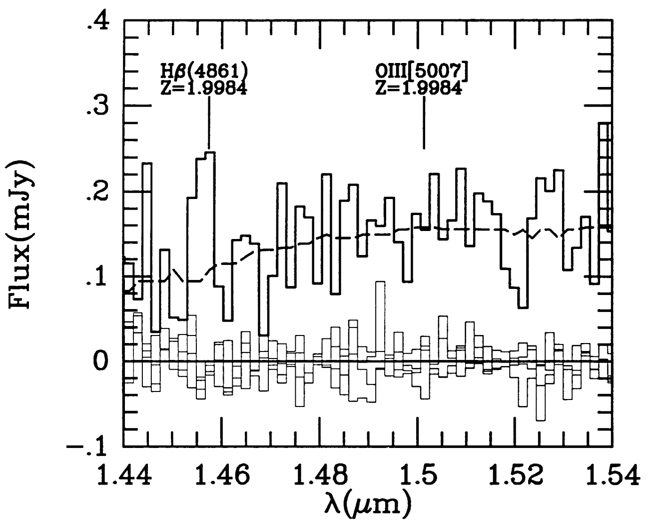

FIG. 2.—Extracted spectra of Q1215+333 obtained with the KPNO 4 m telescope and Cryogenic Spectrometer. Heavy solid line is the quasar spectrum. Heavy dashed line is a median filtered fit to the quasar continuum. The four light lines are spectra extracted on either side of the quasar to illustrate the noise in the spectra. The noise increases blueward of 1.45 μm due to increasing atmospheric absorption. The locations of Hβ and [O III] λ5007 at the redshift of the $z = 2$ damped Lyα absorber are marked. Using the statistics of four pixel averages of the spectra, the Hβ emission line is significant at the 3.8 σ level. No emission is detected at the location of [O III] λ5007.

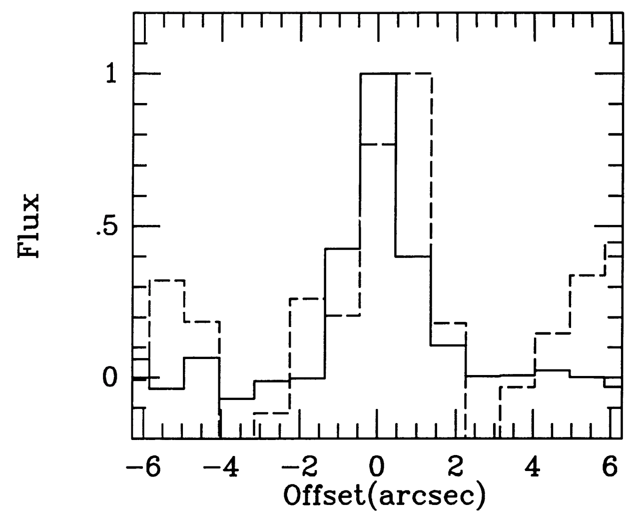

FIG. 3.—Spatial distribution of Hβ emission from the KPNO 4 m observations of the damped Lyα absorber toward Q1215+333. Solid line is the quasar continuum; dashed line is the Hβ emission along a north-south slit centered on the quasar. It appears that the Hβ emission is not resolved. Displacement of the Hβ emission about 1 pixel (0''.9) north of the quasar is not regarded as significant given the signal to noise of the spectra.

Q1215+333 from 110 minutes of on-source observation and 1 hr of sky observation. The extracted spectra of Q1215+333 from the Cryo Spec observations are presented in Figure 2. An unresolved emission line with a flux of $7.6 \pm 2 \times 10^{-16}$ ergs cm^{-2} s^{-1} and a centroid of 1.4560 ± 0.0009 μm is detected at the 4 σ level. This would correspond to a wavelength of 4038 Å in the quasar rest frame ($z_{qso} = 2.606$). We have examined a composite spectrum of the APM quasars (Francis et al. 1991) and find no feature at this wavelength. We propose that this emission feature is due to Hβ emission from the $z = 2$ damped Lyα absorption-line system seen toward this quasar. If we take the redshift of the absorber as 1.9984 (Meyer & Roth 1990), we expect Hβ to appear at 1.4574 μm, 0.0015 ± 0.0009 μm redder than the observed line, or slightly less than 1 pixel. Figure 3 shows the spatial distribution of the Hβ emission. It appears to be unresolved compared to the quasar continuum. It is displaced to the north of the quasar by about 1'', but given the signal to noise of the spectra, a 1 pixel shift is not unexpected. We detect no emission from [O III] λ5007, which would be included in our spectra at 1.501 μm. It occurs near a strong night-sky emission feature, so we take a conservative upper limit for [O III] λ5007 emission of 4×10^{-16} ergs cm^{-2} s^{-1} (2 σ).

Since the Hβ flux detected would imply readily observable Lyα emission, we elected to obtain an independent confirmation of emission from this system. Since [O II] λ3727 should be stronger than Hβ in H II regions where Hβ > [O III] λ5007, we observed the [O II] λ3727 line of the $z = 2$ damped Lyα absorber using the Germanium Spectrometer on the MMT on 1990 May 8. The Ge Spectrometer is a conventional grating spectrometer, utilizing a 2×32 array of Ge photodiodes produced by Ford Aerospace (Rieke et al. 1987). Each diode is coupled to an integrating JFET amplifier with a read noise of about 100 e^-. Using a 600 lines mm^{-1} grating in first order a resolution of 1600 was achieved with a pixel size of 0.0007 μm. Thus the performance of the Ge Spec is roughly equivalent to that of the Cryo Spec, but a one-dimensional spectrum is obtained. We used double 3'' apertures separated by 20''.0 to observe Q1215+333, the quasar in one aperture and sky in the second. The quasar image was alternated between the apertures every 60 s, for a total observation time of 100 minutes. The spectra were sky subtracted using the average of the sky observations taken in the same aperture before and after each 60 s object observation. Finally, the spectra from each aperture were combined using a median algorithm and flattened using observations of the G6 star HR4665.

Figure 4 shows the Ge Spec spectrum of Q1215+333. An emission line centered at 1.1180 ± 0.0004 μm with a flux of $1.6 \pm 0.2 \times 10^{-15}$ ergs cm^{-2} s^{-1} is detected at the 8 σ level.

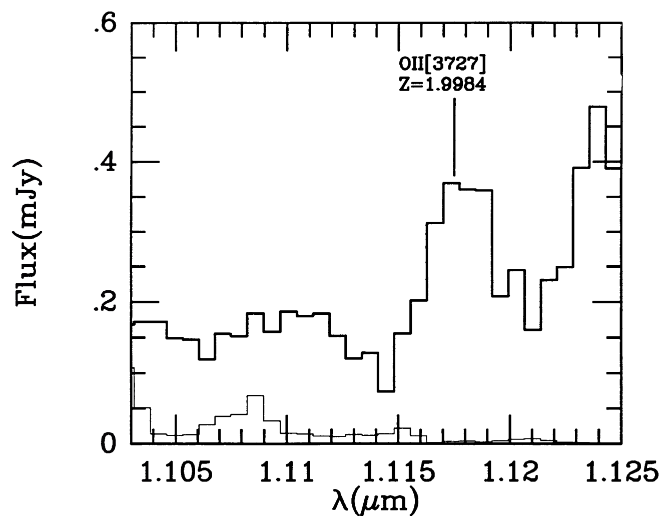

FIG. 4.—Spectrum of Q1215+333 obtained with the Ge Spectrometer on the MMT in 100 minutes. The solid line is the spectrum of the quasar, while the lower line is the night-sky emission divided by a factor of roughly 1000. The location of [O II] λ3727 emission at the redshift of the $z = 2$ damped Lyα absorber toward Q1215+333 is marked. The [O II] emission line is significant at the 8 σ level. The spike of emission at 1.124 μm is not confirmed in a later spectrum and is not regarded as real.

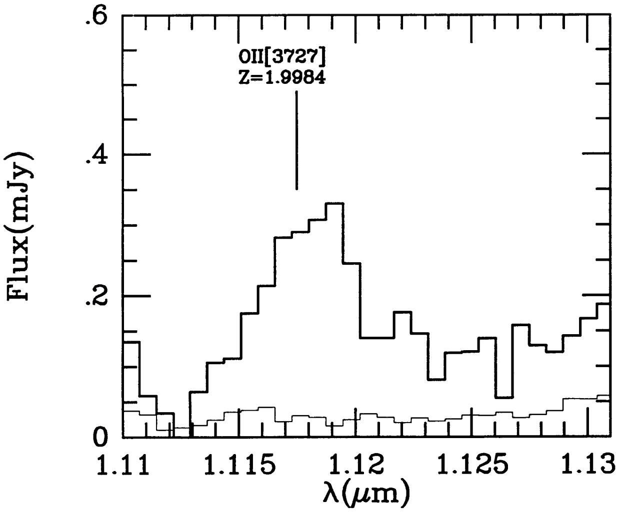

FIG. 5.—Confirming spectrum of [O II] λ3727 emission from the $z = 2$ damped Lyα absorber toward Q1215+333 obtained with the MMT in 45 minutes of observation with the Ge Spectrometer. While at lower signal to noise than the original observation, the [O II] emission appears to be confirmed at the 4 σ level.

Once again we find no emission line at the corresponding rest wavelength (3100 Å) in the composite quasar spectrum. If we identify the observed line as [O II] λ3727 emission from the $z = 1.994$ absorber, the difference between the observed and expected wavelength is 0.0005 ± 0.0004 μm. To confirm this result we reobserved Q1215+333 with the Ge Spec on the MMT on 1990 December 4. This 45 minute confirming observation is shown in Figure 5; once again the emission line is detected, but with lower signal to noise. The confirming observation finds a flux of $2.0 \pm 0.4 \times 10^{-15}$ ergs cm^{-2} s^{-1}, in excellent agreement with the original observation. Within the errors the line position and full width at half-maximum agree with those measured from the original observation. We do not confirm the spike of emission seen in the original spectra at 1.124 μm. We do not regard it as real.

3. DISCUSSION

With our detection of Hβ and [O II] emission from the $z = 2$ damped Lyα absorber toward Q1215+333, we would like to determine the composition of the nebula and source of photoionization. First, the observed ratios [O III] λ5007/Hβ < 0.5 and [O II] λ3727/Hβ = 2 are unlike those seen in AGNs, which have stronger [O III], leaving star formation as the likely source of photoionization (see line classification diagrams of Veilleux & Osterbrock 1987). From the line ratio abundance diagrams of Edmunds & Pagel (1984) we can test if the observed line ratios are consistent with H II regions and derive the nebular abundance. We have two line contraints: log ([O III]/Hβ) ≤ −0.3 and 0.3 ≤ log ([O II] + [O III]/Hβ) ≤ 0.4. The first constraint requires 12 + log (O/H) ≥ 9, while the second constraint requires 8.7 ≤ 12 + log (O/H) ≤ 9.0. Thus it appears that an H II region with 12 + log (O/H) ≈ 9.0 (i.e., approximately solar metallicity) matches the emission-line spectrum of the $z = 2$ damped Lyα absorber in Q1215+333. In local star-forming galaxies with metallicities of 1/10 solar the ratio of [O III] λ5007/Hβ is typically about 10. If the excitation of the nebula associated with the damped Lyα absorber is similar to that in local star-forming galaxies, we can rule out metallicities as low as 1/10 solar very strongly.

The strength of Hβ in this system but weakness of Lyα emission from damped Lyα systems in general is consistent with a solar metallicity star formation region. Hartmann et al. (1988), Deharveng, Joubert, & Kunth (1986), and Meier & Terlevich (1981) noted in low-redshift star-forming galaxies that the Lyα emission is greatly quenched at metallicities in excess of 1/10 solar. This is also consistent with the upper limit on the abundance of nickel obtained by Meyer & Roth (1990), given that nickel may be heavily depleted. A nearly solar abundance of the gas can constrain how far star formation has progressed. If we assume a simple closed box model with instantaneous recycling, we can determine what fraction of the gas has been processed into stars (Tinsely 1980). The yield is uncertain because of the uncertainty in the initial mass function (IMF), but the observed and theoretical values span a range between 0.002 and 0.01 (Peimbert & Serrano 1982). In any case, the oxygen abundance reaches solar when about half the gas has been processed into stars.

Since Hβ is a recombination line, it can be used as a counter of ionizing photons. With the assumption of an IMF and a cosmology we can derive a total star formation rate. Unfortunately, the uncertainty in both the IMF and cosmology is very large; the range of IMF slopes for regions of massive star formation spans $\alpha = -1.0$ to $-2.0[(\partial \log N/\partial \log M) \propto M^{\alpha}]$. Also, the upper and lower mass cutoffs of the assumed IMF have an influence on the conversion from ionizing flux to star formation rate. With the Kennicutt (1983) IMF we find a star formation rate of 140 $M_{\odot}$ yr^{-1} h_{100}^{-2} ($q_0 = 0.5$). We can compare this rate to those derived by Kennicutt, using the same assumptions, for local galaxies. Sbc and Sc galaxies are the most actively star-forming class of objects in Kennicutt's sample with a median star formation rate of 1 $M_{\odot}$ yr^{-1} ($h = 0.5$) and a very small tail extending to about 10 $M_{\odot}$ yr^{-1}. Earlier type galaxies have even lower star formation rates in the Kennicutt sample. This direct comparison indicates a star formation rate over 100 times larger in the $z = 2$ damped Lyα absorber than typical star-forming disk galaxies in the local universe. The Kennicutt IMF has an upper mass power law with $\alpha = -1.5$ and an upper mass limit of 110 $M_{\odot}$. For a flatter power-law IMF ($\alpha = -1.0$) and an upper mass limit of 100 $M_{\odot}$ the star formation rate drops to 30 $M_{\odot}$ yr^{-1} h_{100}^{-2}, while for a steep power-law IMF ($\alpha = -2.0$) and an upper mass limit of 100 $M_{\odot}$, the star formation rate is 430 $M_{\odot}$ yr^{-1} h_{100}^{-2}. This range of IMF slope spans most of the currently observed upper mass slopes of the IMF. For $q_0 = 0$ these star formation rates would increase by a factor of 2.4. In any case for likely values of H_0, q_0, and the IMF slope, the star formation rate is of order 100 $M_{\odot}$ yr^{-1}; with a star formation rate of this magnitude even a galaxy-sized mass of gas would be converted into stars in less than a local Hubble time, indicating we are observing a true "star burst." In a dynamical time scale (10^8 yr) a star formation rate of about 100 $M_{\odot}$ yr^{-1} will produce 10^{10} $M_{\odot}$ in stars. Thus, it seems plausible that we are seeing a star formation episode capable of forming a large fraction of the galaxy's stars.

4. CONCLUSION

We have detected Hβ and [O II] λ3727 emission from the $z = 2$ damped Lyα absorption line system toward Q1215+333. From these observations and the lack of [O III] λ5007 emission we infer a star formation rate of order 100 $M_{\odot}$ yr^{-1} and a metallicity of roughly solar for the star formation region. This result is very different from that inferred from observations of weak Lyα emission from these systems. However, given that Lyα multiply scatters and will be easily quenched by even a small amount of dust, its weakness may not be unexpected. Weak Lyα emission may be indicative of higher metallicity and dust rather than low star formation rates.

While low abundances and small dust contents are inferred for some damped Lyα systems, it may be that since only the brightest quasars are studied, we are selecting only those lines of sight that have low extinction. If we use current day galaxies as analogues, then bright quasars can be seen only through the low-metallicity outer edges of the disk while quasars behind the dusty, metal-enriched inner disk would be dimmed too much to study.

Star formation regions will pollute themselves with metals very rapidly ($<10^7$ yr; Lequeux et al. 1981). Thus their Lyα bright phase may be very short if it terminates when the abundance reaches 1/10 of solar as indicated by local dwarf galaxies. Similarly their dust content will rise rapidly so that lines of sight through star-forming regions may be heavily reddened. Further searches for optical emission which is shifted into the near-IR appear to be the only way to sample the conditions of star formation at high redshift. Given the rapid quenching of Lyα and the resulting bias against lines of sight through dusty, high-metallicity regions, studies in the rest-frame UV will have problems probing these regions.

We plan to observe more systems using near-IR spectroscopy. To date the only other observations have resulted in an upper limit of 4×10^{-16} ergs cm^{-2} s^{-1} for [O II] λ3727 emission from the $z = 2.3$ absorber toward PHL 957. The lack of detectable flux may be due to either lower metal abundance or a lower star formation rate than in the Q1215+333 system. Observations of a Balmer line of hydrogen will show which is the case.

We would like to thank the staffs of the MMT and Kitt Peak National observatories for their assistance in obtaining these observations. R. E. would like to acknowledge the support of a Kitt Peak Post doctoral Fellowship. J. B. acknowledges support from NSF grants RII-8800660 and AST-9058510. J. L. acknowledges the support of a NASA Graduate Student Fellowship. The Ge Spectrometer has been supported by NASA, and NSF grants AST-8715236 and AST-8715373.

REFERENCES

Bergeron, J. 1988, QSO Absorption Lines: Probing the Universe, ed. J. C. Blades, D. Turnshek, & C. A. Norman (Cambridge: Cambridge University Press), 127
Deharveng, J. M., Buat, V., & Bowyer, S. 1990, A&A, 236, 351
Deharveng, J. M., Joubert, M., & Kunth, D. 1986, Star Forming Dwarf Galaxies and Related Objects, ed. D. Kunth, T. X. Thuan, & J. T. T. Van (Paris: Éditions Frontières), 431
Edmunds, M. G., & Pagel, B. E. J. 1984, MNRAS, 211, 507
Fall, S. M., Pei, Y. C., & McMahon, R. G. 1989, ApJ, 341, L5
Foltz, C. B., Chaffee, F. H., & Weymann, R. J. 1986, AJ, 92, 247
Fowler, A. M., & Gatley, I. 1990, ApJ, 353, L33
Francis, P. J., Hewitt, P. C., Foltz, C. B., Chaffee, F. H., & Weymann, R. J. 1991, ApJ, in press
Hartmann, L. W., Huchra, J. P., Geller, M. J., O'Brian, P., & Wilson, R. 1988, ApJ, 326, 101
Hunstead, R. W., Pettini, M., & Fletcher, A. B. 1990, ApJ, 356, 23
Joyce, R. R. 1991, in preparation
Kennicutt, R. C. 1983, ApJ, 272, 54
Lequeux, J., Maucherat-Joubert, M., Deharveng, J. M., & Kunth, D. 1981, A&A, 103, 305
Lowenthal, J. D., Hogan, C. J., Green, R. F., Caulet, A., Woodgate, B. E., Brown, L., & Foltz, C. J. 1991, in preparation
Meier, D. L., & Terlevich, R. 1981, ApJ, 246, L109
Meyer, D. M., & Roth, K. C. 1990, ApJ, 363, 57
Morton, D. C., York, D. G., & Jenkins, E. B. 1988, ApJS, 68, 449
Pei, Y. C., Fall, S. M., & Bechtold, J. 1991, ApJ, in press
Peimbert, M., & Serrano, A. 1982, MNRAS, 198, 563
Rieke, G. H., Elston, R. J., Lebofsky, M. J., & Walker, C. E. 1987, in Infrared Astronomy with Arrays, ed. C. G. Wynn-Williams & E. E. Becklin (Honolulu: University of Hawaii), 69
Smith, H. E., Cohen, R. D., Burns, J. E., Moore, D. J., & Uchida, B. A. 1989, ApJ, 347, 87
Tinsley, B. M. 1980, Fund. Cosmic Phys., 5, 287
Veilleux, S., & Osterbrock, D. E. 1987, ApJS, 63, 295
Wolfe, A. M., Turnshek, D. A., & Lanzetta, K. M. 1990, ApJ, submitted
Yanny, B. 1990, ApJ, 351, 396
Yanny, B., York, D. G., & Williams, T. B. 1990, ApJ, 351, 377